RSC Advances

ROYAL SOCIETY OF CHEMISTRY

www.rsc.org/advances

Cite this: DOI: 10.1039/c0xx00000x

www.rsc.org/xxxxxx

Communication

From macropore to mesopore: diatomite reassembled into a multifunctional composite

Hong-Wen Gao,*[a] Gang Xu,[a] and Yue Wang[a]

Received (in XXX, XXX) Xth XXXX 201X, Accepted Xth XXX 201X

DOI: 10.1039/b000000x

A 'dissolving first and then reassembling' way was presented for preparing a multifunctional composite with diatomite and the antistatic agent SN. The SN@SiO_2 composite binding with sulfonic dye formed the color antistatic agent. Also, it captured nonylphenol from wastewater with the partition coefficient of 5.37×10^4 L/kg and the waste sludge produced was calcined to form the mesoporous sieves.

About twenty countries own the diatomaceous earth mines worldwide. Diatomite reserves is more than two billion tons, where approximately 1% is mined annually[1]. It is fine-grained, low-density biogenic sediment, which consists of amorphous silica ($SiO_2\cdot nH_2O$) derived from opalescent frustules of diatoms[2]. Owing to the advantages of highly porous structure, low density, good stability and low price, diatomite has a wide range of applications, including beer filter aids[3], fabricating porous ceramics[4] and decolorization in food production and wastewater cleanup[5-8]. The waste diatomite is more than 4.7 million tons annually only in Taiwan area[9], either abandoned for polluting environment or disposed cheaply as building filler. Its recycling utilization is the urgent task so as to aviod resource-wasting and environment pollution. Aivalioti *et al* modified diatomite by heat treatment to increase the effective void ratio for raising the adsorption capacity to aromatic compounds[10]. The surface modification of diatomite with ferric oxide improved the removal rate of arsenic[11]. Chaisena *et al* presented the modification with sulphuric acid by the hydrothermal method to successfully prepare sodium zeolite, which can be used as catalyst, ion exchanger, sorbent and water softener[12].

However, the conventional surface modification usually exists some serious defects, for example inapparent improvement of the adsorpriton capacity, easy separation of active groups, difficult reuse and causing secondary pollution[13]. In order to overcome these disadvantages, it is necessary to design a simple process to prepare the cost-effective diatomite composite with the affluent raw materials. This work presented a 'dissolving first and then reassembling' way and it was tried to turn diatomite into a multifunctional composite.

From the infrared spectra (IR) of the composite (Fig. S1 A, ESI†), the Si-O absorption peak changed from 1151 to 1058 cm^{-1}, it may be attributed to the interaction of octadecyl dimethyl hydroxyethyl quaternary ammonium nitrate known as antistatic agent SN (chemically structured in Fig. S1 A, ESI†) with the SiO_2 layer negatively charged. The peaks at 3342, 2922, 2853 and 1383 cm^{-1} indicated that SN is successfully embedded. From the thermal gravimetric analysis (TGA), the loss of weight between 200 and 500 °C indicated approximately 50% SN was hybridized in the SN@SiO_2 composite (Fig. S1 B, ESI†), which accorded with the reaction rate of SN. From the SEM images (Fig. 1A), the composite particles in the size of 100 to 500 nm are irregular and stacked up of the layers, faintly observed (Fig. 1B, Fig. S2, ESI†). From the small angle XRD, the interlayer space is calculated to be 4.4 nm ($2\theta^{001}=2.0^o$) (Fig. 1A), which approaches twice longer than one SN. It may be attributed to the fact that a part of SN formed the layer micelles[14] and SiO_2 grew on surface of the layer.

In addition, a great deal of hollow hexagonal prisms were found in the SN@SiO_2 composite (Fig. 1 B, Fig. S3, ESI†) and all the macropores (>50 nm) disappeared from diatomite (Fig. 1 B, Fig. S4, ESI†). However, no peak appeared in the pore distribution curve (Fig. 1B). Also, the specific surface area of the SN@SiO_2 composite was measured to be 33 m^2/g, where nano pores occupies only 16 m^2/g (Fig. S5, ESI†). It may be attributed to the fact that a part of SN formed the micellar rods[14] at the beginning of the composite preparation. The SiO_2 grew around the SN micellar rods to form the prism framework. In other words, SN was filling into the SiO_2 prism cavity so that N_2 cannot enter, as illustrated in Fig. 1E a. As a result, lots of the SN@SiO_2 prisms were stacked into the layer sheet and the sheets built further into the composite particle.

Owing to enough SN^+ embedded, the SN@SiO_2 composite carries plenty of positive charges, confirmed by the ζ-potential of +44 mV at pH 6.8. It will adsorb sulfonic dye via the opposite charges attraction[15]. The SN@SiO_2 composite was mixed in the aqueous solutions of three lightfast dyes respectively e.g. direct fastlight flavine 5GL, direct fast red F3B and direct fast turquoise blue GL. The dye–SN@SiO_2 products were rapidly formed. The direct fast red F3B–SN@SiO_2 composite were tried to immersed into water for 24 h. The results indicated that less than 0.1% SN and almost no dye stripped from the composite. As an example, the interation of direct fast red F3B with the SN@SiO_2 composite obeyed the Langmuir isotherm model (Fig. S6, ESI†). The saturation binding amounts of direct fast red F3B was calculatd to be 637 mg/g of the composite and its mole ratio to the SN embedding to be 1:3. Two of five sulfonic groups of direct fast red F3B cause the steric effect (chemically structured in Fig. S6, ESI†), thus one dye molecule may bind with at most three SN^+. According to the same method, the carboxyl dyes i.e. eosin Y and

alizarin yellow R were adsorbed and their capacities less than 300 mg/g on the composite, less than those of sulfonic dyes. As a result, the dye molecule entered the SiO_2 prism cavity and bound to the SN's quaternary amine group located on the inside wall of prism, as illustrated in Fig. 1E b.

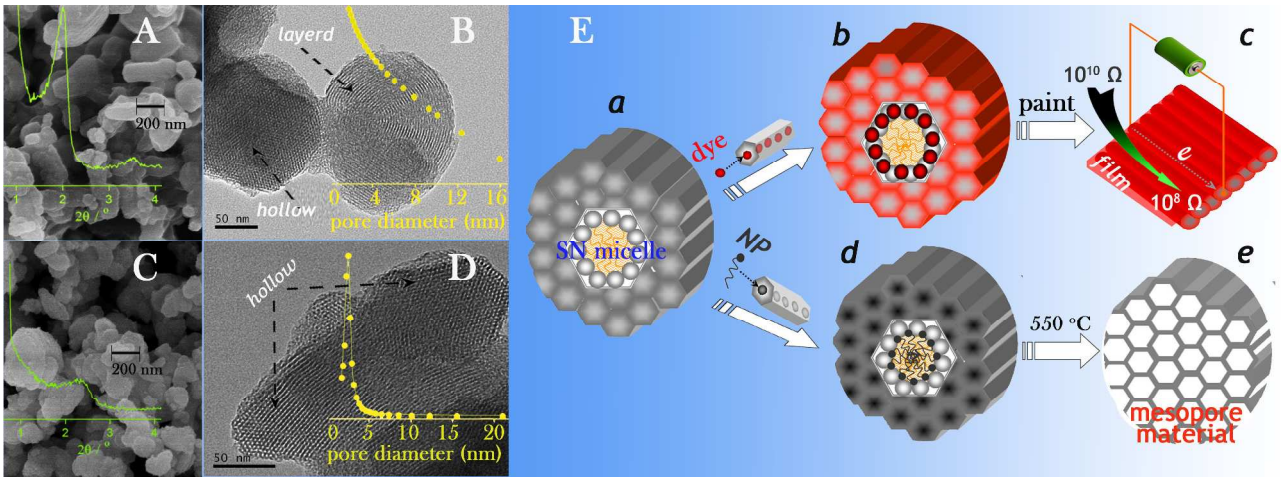

Fig.1 SEM (A, C) and TEM (B, D) images, small angle XRD (curves in A and C) and pore size distribution (curves in B and D) of the materials. A and B: the SN@SiO_2 composite, C and D: the NP-SN@SiO_2 waste calcined. E: Cartoon illustration for 3D structure of the materials / products, a- the SN@SiO_2 composite, b- the composite adsorbing dye, c- the dye-SN@SiO_2 used for preparing the antistatic paint, d- the composite adsorbing NP and e- the NP-SN@SiO_2 waste calcined.

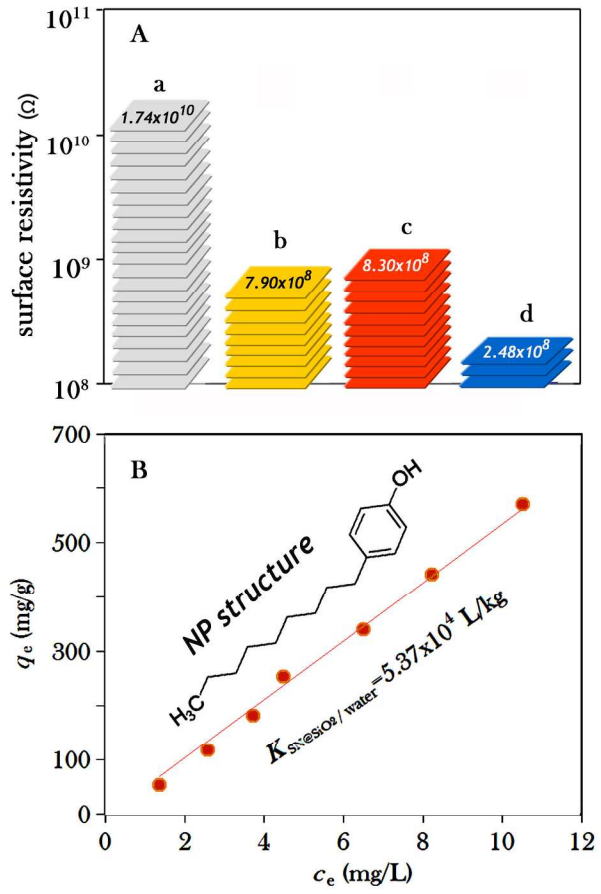

Fig.2 Surface resistivity of the EP - dye-SN@SiO_2 composite films (A) and plots q_e *vs.* c_e of NP solutions treated with 50 mg/L of the SN@SiO_2 composite (B). a: EP-only, b: EP - direct fastlight flavine 5GL-SN@SiO_2, c: EP - direct fast red F3B-SN@SiO_2, and d: EP - direct fast turquoise blue GL-SN@SiO_2.

It is well known that, the electrostatic charges embedding in the plastic and polymer fiber products often bring trouble to people life and even cause the fire or explosion accident in factory and mine. To overcome the problem, various antistatic agents were applied to dissipate the statics[16-18]. As an excellent antistatic agent, SN is most frequently added into the silk, wool and nylon products. The epoxy paint (EP) was tried to prepare the antistatic paint by mixing with only 3% of the dye–SN@SiO_2 composite and coated on the plastic plates. The surface resistivity of the EP-only film (gray) was measured to be 1.74×10^{10} Ω (Fig. 2A), being 21, 20 and 70 times higher than those of the EP – direct fastlight flavine 5GL-SN@SiO_2 film (7.90×10^8 Ω, yellow), the EP - direct fast red F3B-SN@SiO_2 film (8.30×10^8 Ω, red) and the EP - direct fast turquoise blue GL-SN@SiO_2 film (2.48×10^8 Ω, blue). It may be attributed to that SN was filling compactly into the SiO_2 prism to form a weak electrical conductor (Fig. 1E c). The surface resistivity of the EP - dye- SN@SiO_2 films is less than the strict limit, i.e. 1.0×10^9 Ω standardized by U.S. Department of Defense (Documentation No. DOD-HDBK-263) and China National Standard Bureau (No. SJ/T 11294 - 2003). Therefore, the dye–SN@SiO_2 products may be used as the color antistatic agents for adding in the polymer paints e.g. EP and polyurethane.

SN contains a long alkyl chain (Fig. S1 A, ESI†) so that it is able to capture hydrophobic organic compounds e.g. endocrine disrupting chemicals (EDCs). Nonylphenol (NP) is one typical kind of EDCs, jokingly called "sperm killer"[19]. It is usually emitted from chemical wastewater. The EPA's standard indicated NP should be lower than 6.6 μg/L in freshwater. Wastewater containing 4 to 40 mg/L NP was treated with the wet SN@SiO_2 composite prepared above and the result is shown in Fig. 2 B. Without doubt, the adsorption of NP accorded with the partition law. Its partition coefficient ($K_{SN@SiO2/water}$) was calculated to be 5.37×10^4 L/kg, which is 4 times higher than its *n*-octanol/water partition one ($K_{n\text{-octanol/water}} = 1.32\times10^4$ L/kg)[20]. Being different from the above dyes, the hydrophobic NP with a long alkyl chain

(chemically structure in Fig. 2B) may enter the SiO_2 prism center to interact hydrophobically with the alkyl chain of SN, as illustrated in Fig. 1E d. Only 50 mg/L of the SN@SiO_2 composite extracted over 70% NP from its aqueous solution (Fig. S7, ESI†). It is superior to the carbon-base materials in the adsorption speed, capacity and selectivity[21]. It demonstrates that such an adsorption isn't to depend on the specific surface area of material but rather the SN - NP hydrophobic interaction[22]. The SN@SiO_2 composite exhibits a potential applied to treatment of phenolic wastewater.

The spent material i.e. NP-SN@SiO_2 waste was calcined at 550 ^oC. The IR absorption peaks of both SN and NP disappeared and the Si-O peak shifted to 1081 cm^{-1} (Fig. S1 A, ESI†). Undoubtedly, the calcination destroyed the SN and NP structure and their decomposition products escaped from the composite waste. The hexagonal mesopores exposed (Fig. 1D, Fig. S8, ESI†), where only the silica skeleton left, as honeycomb illustrated in Fig. 1E e. The interlayer disappeared from the small angle XRD (Fig. 1C). Such a morphology is similar to the self-assembled materials prepared by the strict design and complicated synthesis[23-25]. N_2 adsorption and desorption isotherm curves (Fig. S5 B, ESI†) showed a typical type IV isotherm with a small H1 hysteresis loop for the calcined product, implying its complexity 2D pore structure. From the pore size distribution curve (Fig. 1D), the most pores appeared at 2.5 nm and mean at 3.7 nm calculated by the BJH method. The specific surface area of the mesoporous silica incresed significantly up to 1066 m^2/g, which is 30 times more than that of the SN@SiO_2 composite. Such a mesoporous sieve is valuable in gas adsorption, catalyst, heat insulation and the other fields[26-30].

This work suggested a simple preparation process of the multifunctional diatomite composite from alkali dissolution and acid neutralization to SN coprecipitation. Such an in-depth functionalization is essentially different from the conventional surface modification[11,12,31,32]. The performance of the SN@SiO_2 composite gets a significant raise, e.g. the active group SN firmly embedded, high adsorption capacity and rapid adsorption equilibrium to sulfuric dye and NP. It can bind with sulfonic dyes to prepare the excellent color antistatic agents, and use as the outstanding sorbent for remediation of water contaminated by organic pollutants. Furthermore, preparing a potentially valuable mesoporous sieve realized the resource-oriented utilization of the diatomite waste and the possible secondary pollution is avoided. In brief, the 'dissolving first and then reassembling' way will make waste profitable.

The authors acknowledge the financial support from The Foundation of State Key Laboratory of Pollution Control and Resource Reuse (Tongji University), China (Grant No. PCRRK11003).

Notes and references

[a] *State Key Laboratory of Pollution Control and Resource Reuse, College of Environmental Science and Engineering, Tongji University, Shanghai 200092, China. Fax: 86-21-65988598; Tel: 86-21-65988598; E-mail: hwgao@tongji.edu.cn*

† Electronic Supplementary Information (ESI) available: Experimental details and Fig. S1 to S8. See DOI:10.1039/b000000x/

1 H. Hadjar, B. Hamdi, M. Jaber, J. Brendie, Z. Kessaissia, H. Balard and J. B. Donnet, *Micropor. Mesopor. Mater.*, 2008, **107**, 219.
2 G. Sheng, S. Yang, J. Sheng, J. Hu, X. Tan and X. Wang, *Environ. Sci. Technol.*, 2011, **45**, 7718.
3 S. Martinovic, M. Vlahovic, T. Boljanac and L. Pavlovic, *Int. J. Miner. Process.*, 2006, **80**, 255.
4 K. L. Lin, T. C. Lee, J. C. Chang and J. Y. Lan, *Environ. Prog. Sustain. Energy*, 2013, **32**, 640.
5 M. A. Khraisheh, M. A. Al-Ghouti, S. J. Allen and M. N. Ahmad, *Water Res.*, 2005, **39**, 922.
6 M. Jang, S. H. Min, T. H. Kim and J. K. Park, *Environ. Sci. Technol.*, 2006, **40**, 1636.
7 R. Knoerr, J. Brendlé, B. Lebeau and H. Demais, *New J. Chem.*, 2011, **35**, 461.
8 O. Hernández-Ramírez, P. I. Hill, D. J. Doocey and S. M. Holmes, *J. Mater. Chem.*, 2007, **17**, 1804.
9 K. L. Lin, J. C. Chang, J. L. Shie, H. J. Chen and C. M. Ma, *Environ. Eng. Sci.*, 2012, **29**, 436
10 M. Aivalioti, P. Papoulias, A. Kousaiti and E. Gidarakos, *J. Hazard. Mater.*, 2012, **207**, 117.
11 Y. Du, H. Fan, L. Wang, J. Wang, J. Wu and H. Dai, *J. Mater. Chem. A*, 2013, **1**, 7729.
12 A. Chaisena and K. Rangsriwatananon, *Mater. Lett.*, 2005, **59**, 1474.
13 M. A. M. Khraisheh, Y. S. Al-Degs and W. A. M. McMinn, *Chem. Eng. J.*, 2004, **99**, 177.
14 J. L. Anderson, V. Pino, E. C. Hagberg, V. V. Sheares and D. W. Armstrong, *Chem. Commun.*, 2003, 2444; Y. P. Wei, H. W. Gao, *J. Mater. Chem.*, 2012, **22**, 5715.
15 D. H. Zhao, Y. L. Zhang, Y. P. Wei and H. W. Gao, *J. Mater. Chem.*, 2009, **19**, 7239; G. Xu, H. W. Gao, *Acta Chim. Sinica*, 2012, **70**, 2496; Z. Y. Chen, H. W. Gao, Y. Y. He, *RSC Adv.*, 2013, **3**, 5815.
16 D. V. Andreeva and D. G. Shchukin, *Mater. Today*, 2008, **11**, 24.
17 C. S. Li, T. X. Liang, W. Z. Lu, C. H. Tang, X. Q. Hu, M. S. Cao and J. Liang, *Compos. Sci. Technol.*, 2004, **64**, 2089.
18 M. Radetic, *J. Mater. Sci.*, 2013, **48**, 95.
19 T. Negishi, K. Kawasaki, S. Suzaki, H. Maeda, Y. Ishii, S. Kyuwa, Y. Kuroda and Y. Yoshikawa, *Environ. Health Perspect.*, 2004, **112**, 1159.
20 X. L. Li, T. G. Luan, Y. Liang, M. H. Wong and C. Y. Lan, *J. Environ. Sci.*, 2007, **19**, 657.
21 H. Y. Niu, Y. X. Wang, X. L. Zhang, Z. F. Meng and Y. Q. Cai, *ACS Appl. Mater. Inter.*, 2012, **4**, 286-295.
22 P. Wang, Q. H. Shi, Y. F. Shi, K. K. Clark, G. D. Stucky and A. A. Keller, *J. Am. Chem. Soc.*, 2009, **131**, 182.
23 S. D. Shen, A. E. Garcia-Bennett, Z. Liu, Q. Y. Lu, Y. F. Shi, Y. Yan, C. Z. Yu, W. C. Liu, Y. Cai, O. Terasaki and D. Y. Zhao, *J. Amer. Chem. Soc.*, 2005, **127**, 6780.
24 Y. Wan, Y. Shi and D. Zhao, *Chem. Commun.*, 2007, 897.
25 C. Gérardin, J. Reboul, M. Bonne and B. Lebeau, *Chem. Soc. Rev.*, 2013, **42**, 4217.
26 E. P. Ng, D. Chateigner, T. Bein, V. Valtchev and S. Mintova, *Science*, 2012, **335**, 70.
27 J. Kim, L. C. Lin, J. A. Swisher, M. Haranczyk and B. Smit, *J. Amer. Chem. Soc.*, 2012, **134**, 18940.
28 Y. Q. Dai, B. Lim, Y. Yang, C. M. Cobley, W. Y. Li, E. C. Cho, B. Grayson, P. T. Fanson, C. T. Campbell, Y. M. Sun and Y. N. Xia, *Angew. Chem.-Int. Edit.*, 2010, **49**, 8165.
29 J. Zhou, Z. Hua, X. Cui, Z. Ye, F. Cui and J. Shi, *Chem. Commun.*, 2010, 4994.
30 C. T. Kresge and W. J. Roth, *Chem. Soc. Rev.*, 2013, **42**, 3663.
31 O. Hernandez-Ramireza and S. M. Holmes, *J. Mater. Chem.*, 2008, **18**, 2751.
32 B. Bahramiana, F. D. Ardejanib, V. Mirkhanic and K. Badiid, *Appl. Catal. A - Gen.*, 2008, **345**, 97.